Certifiably Correct Range-Aided SLAM

Alan Papalia[1,2], Andrew Fishberg[1], Brendan W. O'Neill[1,2], Jonathan P. How[1],
David M. Rosen[3], John J. Leonard[1]

[1] Massachusetts Institute of Technology   [2] Woods Hole Oceanographic Institution
[3] Northeastern University

Abstract—We present the first algorithm capable of efficiently computing certifiably optimal solutions to range-aided simultaneous localization and mapping (RA-SLAM) problems. Robotic navigation systems are increasingly incorporating point-to-point ranging sensors, leading state estimation which takes the form of RA-SLAM. However, the RA-SLAM problem is more difficult to solve than traditional pose-graph SLAM; ranging sensor models introduce additional non-convexity, unlike pose-pose or pose-landmark measurements, a single range measurement does not uniquely determine the relative transform between the involved sensors, and RA-SLAM inference is highly sensitive to initial estimates. Our approach relaxes the RA-SLAM problem to a semidefinite program (SDP), which we show how to solve efficiently using the Riemannian staircase methodology. The solution of this SDP provides a high-quality initialization for our original RA-SLAM problem, which is subsequently refined via local optimization, as well as a lower-bound on the RA-SLAM problem's optimal value. Our algorithm, named certifiably correct RA-SLAM (CORA), applies to problems comprised of arbitrary pose-pose, pose-landmark, and ranging measurements. Evaluation on simulated and real-world marine examples shows that our algorithm frequently produces certifiably optimal RA-SLAM solutions; moreover, even suboptimal estimates are typically within 1-2% of the optimal value.

I. INTRODUCTION

Range-aided simultaneous localization and mapping (RA-SLAM) is a state estimation task with application domains spanning underwater [1, 2], in air [3], underground [4], and planetary [5] environments. RA-SLAM extends standard pose-graph SLAM [6, 7] with point-to-point range measurements, enabling sensor modalities not found in pose-graph SLAM. Range sensing possesses notable advantages, as measurements often have known data-association and in many environments (e.g., underwater) range measurements are critical to long-term positional estimation. Despite the broad applicability of RA-SLAM and the advantages of range sensing, RA-SLAM approaches lack the optimality guarantees and robustness to initialization found in modern pose-graph SLAM [8].

The difficulties surrounding RA-SLAM arise from the problem structure. RA-SLAM is often posed as *maximum a posteriori* estimation, leading to a nonlinear least-squares (NLS) problem [9, 10]. As the NLS formulation is non-convex, standard approaches only guarantee locally optimal solutions and cannot distinguish local from global optimality. These issues have been circumvented in pose-graph SLAM [8]. However, range sensing introduces additional non-convexity to the cost function which prevents application of these techniques.
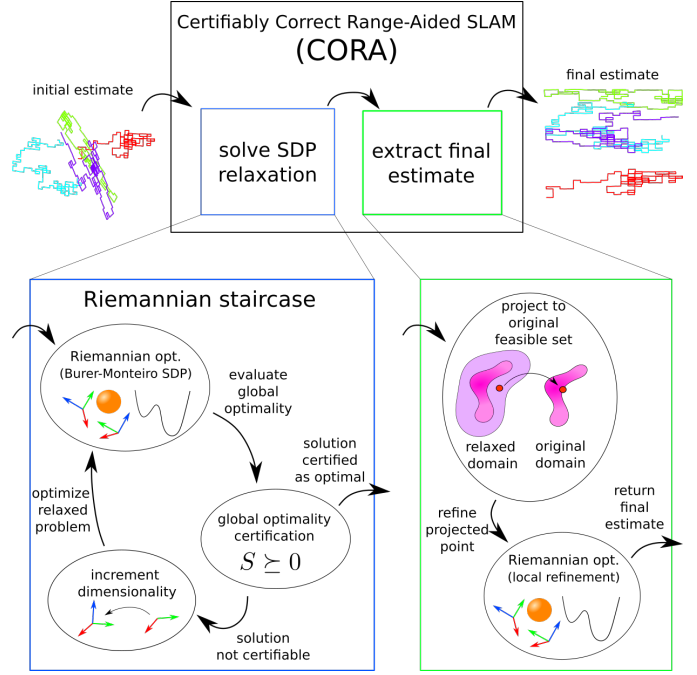

Fig. 1. A schematic overview of the proposed algorithm on a four robot RA-SLAM problem. (Top) the high-level flow, which takes an initial estimate solves a semidefinite program (SDP) relaxation of the RA-SLAM problem. As the SDP solution is not necessarily feasible for the RA-SLAM problem, a final estimate to the original problem is then extracted and returned. (Bottom-Left) The Riemannian staircase methodology used to solve the SDP, in which a optimization is performed over increasingly lifted Riemannian optimization problems until a certified solution to the SDP is found. The Riemannian optimization is over a product manifold involving orthonormal frames and vectors on the unit-sphere, certification involves evaluating positive semidefiniteness of a specific matrix, and lifting is equivalent to increasing the dimensions of the product manifold. (Bottom-Right) extracting the final estimate via feasible set projection followed by Riemannian optimization.

This work presents CORA, an algorithm capable of returning certifiably optimal estimates to the RA-SLAM problem. We establish connections between RA-SLAM, SDPs, and Riemannian optimization to develop efficient methodologies for RA-SLAM state estimation and solution certification.

CORA solves an SDP relaxation of the RA-SLAM problem to obtain a lower bound on the optimal value of the original RA-SLAM problem and an initialization to a local optimization approach. To improve the scalability of solving this SDP, we demonstrate that the feasible set of the Burer-Monteiro-factored SDP [11, 12] admits a Riemannian interpretation, and apply the Riemannian staircase approach [13, 14]. Importantly, we construct a certification scheme to determine if a given

estimate solves the SDP. This certification scheme leverages analysis of the Karush-Kuhn-Tucker (KKT) conditions of the SDP [15] to reduce optimality verification to a series of sparse linear algebraic operations. Finally, the SDP solution is projected to the feasible set of the original RA-SLAM problem and locally optimized to produce a final estimate and an upper bound on the suboptimality of the estimate.

We evaluate CORA on (1) two marine platforms equipped with inertial sensing and acoustic modems for ranging and (2) simulated RA-SLAM problems. We demonstrate that CORA often obtains certifiably optimal solutions to realistic RA-SLAM scenarios. Moreover, in instances when the solution is not *exactly* optimal, it typically achieves an objective value within 1-2% of the lower bound

We summarize the contributions of this paper as follows:

- The first RA-SLAM algorithm capable of producing certifiably optimal estimates.
- An open-source implementation, including all experimental data presented in this paper[1].

Additionally, we consider several proofs contained in Appendix D as minor contributions of independent interest.

II. RELATED WORKS

Certification in robotic perception typically describes a certificate of optimality of some estimated quantity, where the estimation procedure is defined as an optimization problem [15, 16, 17]. Works in certifiable estimation generally are either an optimizer paired with a global optimality certification scheme or an exhaustive search approach.

A. Sufficient Conditions for Global Optimality

Many certification schemes leverage relationships between quadratically constrained quadratic programs (QCQPs) and SDPs to construct KKT-based certifiers. These certifiers establish sufficient conditions for optimality which, if satisfied, guarantee global optimality [15, 18, 19]. Broadly, certifiable perception approaches fall under the class of probably certifiably correct algorithms, as described by Bandeira [17].

Additionally, works in certification can be separated by the estimation methodology proposed; works typically pair a certifier with a local-optimizer or a SDP relaxation. The SDP approaches solve a relaxation of the original problem and then project the relaxed solution to the feasible set of the original problem. In general, both approaches can obtain optimal solutions but do not *guarantee* such. Notable SDP-based works [8, 20] established conditions when such guarantees exist. Importantly, unlike local optimization, the estimates from SDP methods are initialization-dependent.

Local-optimization approaches: KKT-based sufficient conditions were derived from various QCQPs and paired with local optimizers to solve problems in point-cloud registration [21, 22], multi-view geometry [23], pose-graph SLAM [24, 25], and range-only localization [26]. In addition to KKT-based certificates, a number of computer vision works

developed certification schemes based on proving problem convexity over the feasible set [27, 28, 29].

SDPs and Interior Point Methods: Many approaches in robotic perception formulate problems as a QCQP, solve an SDP relaxation of the QCQP [30], and then project the SDP solution to the feasible set of the original problem. Often the SDP relaxation is exact, and thus the projection is a certifiably optimal solution to the original problem. Previous approaches applied standard SDP solvers to problems in geometric registration [31, 32, 33], robust point-cloud registration [34], relative pose estimation [35, 36], triangulation [37], anonymous bearing-only multi-robot localization [38], essential matrix estimation [39], pose-graph SLAM [40], and sensor calibration [41]. While standard interior point methods scale poorly for large problems, these approaches are successful on small problems and can use a broad set of solvers.

SDPs and the Riemannian staircase: SDP relaxations of robotic perception problems typically admit low-rank solutions. A growing body of work applies the Riemannian staircase methodology [13, 14] to leverage this low-rank structure and more efficiently solve the SDP. Riemannian staircase approaches differ from the previously mentioned SDP approaches in that they (1) optimize over a series of lower-dimension, non-convex, rank-restricted SDPs to solve the original SDP and (2) Riemannian optimization techniques are used to enhance the rank-restricted SDP optimization. Importantly, while the approach of solving a series of rank-restricted SDPs can be applied to all SDPs [11, 12, 15], usage of Riemannian optimization depends on specific problem structure and does not apply to all SDPs. Within robotics, the Riemannian staircase has been applied to pose-graph SLAM [8, 42, 43] and range-only localization [44].

Placement of this Work: This work falls under the Riemannian staircase class of works. We present a SDP formulation, certification procedure, Riemannian staircase methodology, and means for extracting a solution from the SDP solution. Our work differs from recent, important papers in certification for the closely related problem of range-only localization [26, 44], as a novel problem formulation and certification methodology were necessary to account for pose variables. Our certification approach builds upon the KKT-based analyses of [15, 18]. Additionally, our problem formulation and estimation procedure generalize similar, key works in range-only localization [44] and pose-graph SLAM [8, 42] to the case of RA-SLAM.

B. Exhaustive Search

Exhaustive search approaches largely use either polynomial root finding or branch-and-bound (BnB) techniques to guarantee a globally optimal solution will be found [45, 46]. Such *a priori* guarantees typically cannot be made for other approaches. These approaches come at increased computational cost, particularly as problem sizes increase.

Polynomial solving via Gröbner basis computation was applied to multi-view geometry [47, 48] and range-only localization [49]. Similarly, [50] solved a polynomial system via eigendecomposition to estimate relative camera pose.

BnB was applied to consensus maximization in rotation search [51] and special Euclidean registration [52]. [53] linearly approximated $SO(3)$ to solve pose estimation as a mixed-integer convex program for improved BnB efficiency. Similarly, [54] integrated the iterative closest point solver into a BnB framework to efficiently perform point cloud registration. BnB was also applied to the estimation of: camera focal length and relative rotation [55], correspondence-free relative pose [56, 57], essential matrices [58, 59], and triangulation [60].

III. RA-SLAM AS AN SDP

In this section we demonstrate how the *maximum a posteriori* (MAP) formulation of RA-SLAM can be used to derive a novel SDP. This SDP will underpin many of the key contributions of this work. The MAP formulation is based on generative measurement models with Langevin distributed rotational noise and Gaussian distributed translational and ranging noise. We present these models as,

$$\tilde{R}_{ij} = \underline{R}_{ij}R_{ij}^{\epsilon}, \qquad R_{ij}^{\epsilon} \sim \text{Langevin}\,(I_d, \kappa_{ij}) \quad (1)$$

$$\tilde{t}_{ij} = \underline{t}_{ij} + t_{ij}^{\epsilon}, \qquad t_{ij}^{\epsilon} \sim \mathcal{N}\left(0, \tau_{ij}^{-1}I_d\right) \quad (2)$$

$$\tilde{r}_{ij} = \|\underline{t}_i - \underline{t}_j\|_2 + r_{ij}^{\epsilon}, \qquad r_{ij}^{\epsilon} \sim \mathcal{N}\left(0, \sigma_{ij}^2\right) \quad (3)$$

where $\tilde{R}_{ij}, \tilde{t}_{ij}, \tilde{r}_{ij}$ are noisy relative rotational, translational, and range measurements. Similarly, $\underline{R}_{ij}, \underline{t}_{ij}, \underline{r}_{ij}$ are the true relative rotations, translations, and ranges. Finally, $R_{ij}^{\epsilon}, t_{ij}^{\epsilon}, r_{ij}^{\epsilon}$ represent the noisy perturbations to the measurements where the coefficients κ_{ij}, τ_{ij}, and $(1/(\sigma_{ij}^2))$ are, respectively, the rotational, translational, and ranging measurement precisions.

From the measurement models of Eqs. (1) to (3) the MAP formulation of RA-SLAM is as follows [61],

Problem 1 (MAP formulation of RA-SLAM). *Given sets of relative pose measurements,* $\{\tilde{R}_{ij}, \tilde{t}_{ij}\}_{(i,j)\in\mathcal{E}_p}$*, and of distance measurements,* $\{\tilde{r}_{ij} \in \mathbb{R}\}_{(i,j)\in\mathcal{E}_r}$ *find the problem variables,* $\{R_i, t_i\}_{i=1}^n$ *, which solve*

$$\min_{\substack{R_i \in \text{SO(d)} \\ t_i \in \mathbb{R}^d}} \quad \sum_{(i,j)\in\mathcal{E}_p} \kappa_{ij}\|R_j - R_i\tilde{R}_{ij}\|_F^2$$
$$+ \sum_{(i,j)\in\mathcal{E}_p} \tau_{ij}\left\|t_j - t_i - R_i\tilde{t}_{ij}\right\|_2^2 \quad (4)$$
$$+ \sum_{(i,j)\in\mathcal{E}_r} \frac{1}{\sigma_{ij}^2}(\|t_j - t_i\|_2 - \tilde{r}_{ij})^2$$

where $\mathcal{E}_p$ *and* $\mathcal{E}_r$ *are the sets of edges representing relative pose measurements and range measurements, respectively. Additionally,* d *is the dimension of the problem (e.g., 2D or 3D) and* n *is the number of pose variables.*

From Problem 1 we derive a relaxed problem, which takes the form of a QCQP and, in turn, leads to a convenient SDP relaxation. This QCQP (Problem 2) relaxes the special orthogonal constraint ($R_i \in \text{SO(d)}$) to an orthogonality constraint ($R_i \in \text{O(d)}$). This relaxation was found to have no impact on typical pose-graph SLAM solution quality [8, 42, 62].

Additionally, the range cost terms of Problem 1 are modified. We introduce auxiliary unit-norm vector variables ($r_{ij} \in$

S^{d-1}, where S^{d-1} is the d-dimensional unit sphere). This reformulation of the range cost terms in Problem 2 is equivalent to the terms presented in Problem 1 in the sense that optimal solutions are identical [44, Lemma 1].

We present this relaxation in Problem 2, noting that all costs and constraints are quadratic.

Problem 2 (QCQP relaxation of RA-SLAM). *Given the measurements of Problem 1, find the variables,* $\{R_i, t_i\}_{i=1}^n \cup \{r_{ij}\}_{(i,j)\in\mathcal{E}_r}$ *, which solve:*

$$\min_{\substack{R_i \in \mathbb{R}^{d\times d} \\ t_i \in \mathbb{R}^d \\ r_{ij} \in \mathbb{R}^d}} \quad \sum_{(i,j)\in\mathcal{E}_p} \kappa_{ij}\|R_j - R_i\tilde{R}_{ij}\|_F^2$$
$$+ \sum_{(i,j)\in\mathcal{E}_p} \tau_{ij}\left\|t_j - t_i - R_i\tilde{t}_{ij}\right\|_2^2 \quad (5)$$
$$+ \sum_{(i,j)\in\mathcal{E}_r} \frac{1}{\sigma_{ij}^2}\|t_j - t_i - \tilde{r}_{ij}r_{ij}\|_2^2$$
$$\text{subject to} \quad R_i^\top R_i = I_d, \ i = 1, \dots, n$$
$$\|r_{ij}\|_2^2 = 1, \ \forall(i,j)\in\mathcal{E}_r \ .$$

Furthermore, we note that any QCQP can be relaxed to an SDP via Shor's relaxation [63]. This SDP relaxation of Problem 2 takes the form of,

Problem 3 (SDP relaxation of RA-SLAM). *Find* $Z \in \mathbb{R}^{k\times k}$ *that solves*

$$\min_{Z \in \mathbb{R}^{k\times k}} \quad \text{tr}(QZ)$$
$$\text{subject to} \quad \text{tr}(A_i Z) = b_i, \quad i = 1, \dots, m \quad (6)$$
$$Z \succeq 0.$$

where $k \triangleq n(d+1) + l$ *and* $l \triangleq |\mathcal{E}_r|$ *is the number of range measurements.* $Q \in \mathcal{S}_+^k$*, and* $A_i \in \mathbb{R}^{k\times k}$ *are real, symmetric,* $k \times k$ *matrices defined in Appendices B and C.* $\mathcal{S}_+^k$ *defines the set of* $k \times k$ *positive semidefinite matrices.*

The key contributions of this work stem from Problem 3, which is convex and thus admits several critical properties. The SDP of Problem 3 is a strict relaxation of the original problem in Problem 1. Thus, a solution to the SDP provides both a principled initialization to the original problem and a lower bound on the optimal cost of the original problem.

However, in this work we do not solve the SDP of Problem 3 in its existing form. We instead apply the Burer-Monteiro method to take advantage of the expected low-rank solution to Problem 3. We substitute $Z = XX^\top, X \in \mathbb{R}^{k\times p}$ to arrive at a rank-restricted SDP of the form:

Problem 4 (Burer-Monteiro factorization of Problem 3). *Find* $X \in \mathbb{R}^{k\times p}$ *that solves*

$$\min_{X \in \mathbb{R}^{k\times p}} \quad \text{tr}(QXX^\top)$$
$$\text{subject to} \quad \text{tr}(A_i XX^\top) = b_i, \quad i = 1, \dots, m. \quad (7)$$

In this rank-restricted SDP the problem variable, X, is

composed as follows,

$$T_i \in \mathbb{R}^{p \times (d+1)} \triangleq [R_i \mid t_i] \tag{8}$$

$$X \in \mathbb{R}^{k \times p} \triangleq [T_1 \mid \cdots \mid T_n \mid r_1 \mid \cdots \mid r_l]^\top \tag{9}$$

where each element, e.g., $R_i \in \mathbb{R}^{p \times d}$, can be considered a natural lifting of the variables in the QCQP of Problem 2, e.g., $R_i \in \mathbb{R}^{d \times d}$, when $p > d$. Furthermore, the rank-restricted SDP of Problem 4 is equivalent to the QCQP of Problem 2 when $p = d$. Importantly, p constrains the rank of the solution to Problem 4, as $\text{rank}(X) = \text{rank}(XX^\top) \leq p$.

From these observations, it follows that incrementing p provides an interpretable means of relaxing Problem 4 by increasing the allowable rank of the solution. This relaxation methodology is a key aspect to our estimation procedure.

IV. DERIVING THE OPTIMALITY CERTIFICATES

In this section we demonstrate how previous results in certifiable estimation [15] can be applied to Problem 4. This approach centers around the *certificate matrix*, S, which relates the rank-restricted SDP of Problem 4 to the SDP of Problem 3. Specifically, if a S obtained from a candidate solution, X^*, to Problem 4 is positive semidefinite, then X^* solves Problem 3 and must be optimal for Problem 4.

Critically, our approach to obtaining S requires that the linear independence constraint qualification (LICQ) is satisfied. We discuss the LICQ and its relationship to S and then describe our algorithm for performing certification.

A. The Linear Independence Constraint Qualification

The certificate matrix we devise is a function of the Lagrange multipliers (λ_i) at a given solution point (X^*). However, to guarantee a unique set of Lagrange multipliers the LICQ must be satisfied [64]. Without satisfying the LICQ there is no guarantee that the computed Lagrange multipliers will lead to a PSD certificate matrix [15, footnote 3].

The LICQ requires that the set of gradients of the constraints is linearly independent. For Problem 4, the LICQ is equivalent to linear independence of $\{\nabla_X \text{tr}(A_i XX^\top), \quad i = 1, \ldots, m\}$ evaluated at $X = X^*$. This condition is equivalent to the following *constraint gradient matrix*,

$$K \in \mathbb{R}^{(kd) \times m} \triangleq [\text{vec}(A_1 X^*) \mid \cdots \mid \text{vec}(A_m X^*)] \tag{10}$$

having full column rank, where $\text{vec}(\cdot)$ is the columnwise vectorization operator.

We ensure that for our application the LICQ will always be satisfied (Theorem 1).

Theorem 1 (LICQ for Problem 4). *The LICQ is satisfied for any feasible point, X, of Problem 4.*

Proof: See Appendix D.

B. Performing Certification

In this section we demonstrate how solution certification is reduced to three steps: (1) solving a single linear least-squares problem, (2) matrix addition, (3) and evaluating positive semidefiniteness of a real, symmetric matrix. All matrices in these computations are sparse, enabling efficient computation.

Our certification scheme first computes a certificate matrix, S, and then evaluates if $S \succeq 0$. Following the presentation of [15], the certificate matrix can be written as:

$$S \triangleq Q + \sum_{i=1}^m \lambda_i A_i \tag{11}$$

where λ_i is the Lagrange multiplier corresponding to the constraint A_i.

Computing Lagrange Multipliers: As the Lagrange multipliers are a function of the specific solution point evaluated, they must be computed for each candidate solution. By the stationarity condition of the KKT conditions, we determine the Lagrange multipliers via a linear least-squares problem. For any stationary point, the partial derivative of the Lagrangian with respect to the problem variable is zero [65, Theorem 12.1]. Gathering the Lagrange multipliers as a vector, $\lambda \in \mathbb{R}^m \triangleq [\lambda_1, \ldots, \lambda_m]$, the partial derivative of the Lagrangian of Problem 4 is

$$\partial_X \mathcal{L}(X, \lambda) = \partial_X \text{tr}(QXX^\top)$$
$$+ \partial_X \sum_{i=1}^m (\text{tr}(A_i XX^\top) - b_i)\lambda_i \tag{12}$$
$$= 2QX + 2(\sum_{i=1}^m A_i \lambda_i)X.$$

It follows from Eq. (12) that the first-order stationarity condition of Problem 4 is,

$$QX^* + (\sum_{i=1}^m A_i \lambda_i)X^* = \mathbf{0}, \tag{13}$$

where $X^* \in \mathbb{R}^{k \times p}$ is a stationary point of Problem 4 and $\mathbf{0}$ is the zero matrix.

Observe that Eq. (13) is linear with respect to the Lagrange multipliers. We rearrange Eq. (13) to arrive at

$$\sum_{i=1}^m (A_i X^*)\lambda_i = -QX^*. \tag{14}$$

By vectorizing each side of Eq. (14) we arrive at

$$K\lambda = -\text{vec}(QX^*) \tag{15}$$

where K is the constraint gradient matrix of Eq. (10). Thus, the Lagrange multipliers, λ, may be estimated by solving the linear system of Eq. (15).

Building S and Evaluating Optimality: Given the Lagrange multipliers, λ, the certificate matrix can be formed as in Eq. (11). By [15, Theorem 4], if $S \succeq 0$, the candidate solution, X^*, is globally optimal. For this problem, the most efficient means of checking $S \succeq 0$ is by attempting to Cholesky factorize $S + \beta I$, where $0 < \beta \ll 1$. Cholesky factorization requires positive definite matrices, and thus β is a numerical tolerance parameter for the positive semidefiniteness of S. We summarize this certification scheme in Algorithm 1.

Algorithm 1 Certify Optimality of a Candidate Solution, X^*

Input: the solution to certify $X^* \in \mathbb{R}^{k \times p}$, positive semidefinite tolerance parameter $\beta \in \mathbb{R}_{++}$
Output: whether X^* is globally optimal
Require: X^* is locally optimal
  function ISOPTIMAL(X^*, β)
    $\lambda \leftarrow$ solve the linear system of Eq. (15)
    $S \leftarrow Q + \sum_{i=0}^m \lambda_i A_i$
    try Cholesky$(S + \beta I)$
      return is_optimal = True
    catch $S + \beta I$ not positive definite
      return is_optimal = False

Algorithm 2 Certifiably Correct RA-SLAM

Input: an initial estimate $X_0 \in \mathbb{R}^{k \times p}$
Output: an estimate, X^*
  function CORA(X_0)
    $\beta \leftarrow 10^{-8}$
    $X^* \leftarrow X_0$
    certified $\leftarrow$ isOptimal(X^*, β)
    while not certified **do**
      // lift X^* by appending a column
      // and adding a small perturbation[2]
      $X^* \leftarrow [X^* \mid \delta]$
      $X^* \leftarrow$ RiemannianOpt(X^*, Q)
      certified $\leftarrow$ isOptimal(X^*, β)
    end
    $X^* \leftarrow$ ProjectSolution(X^*, d) ▷ [8, Algorithm 2]
    $X^* \leftarrow$ RiemannianOpt(X^*, Q)
    return X^*

V. CERTIFIABLY CORRECT ESTIMATION

In this section we describe our approach to certifiably correct estimation. We demonstrate that the rank-restricted SDP of Problem 4 can be solved via Riemannian optimization, enabling use of the Riemannian staircase methodology. We then describe the Riemannian staircase as applied to Problem 4 and discuss how we use the Riemannian staircase estimate to extract an estimate to the original problem, Problem 1.

A. Problem 4 as Riemannian Optimization

We consider the variable $X \in \mathbb{R}^{k \times p}$ as described in Eq. (9). The constraints imposed on X by the A_i of Problem 4 are equivalent to the quadratic equality constraints described in the QCQP of Problem 2. Specifically, $R_i^\top R_i = I_d$ and $\|r_{ij}\|_2^2 = 1$.

Through this lens, we show that the feasible set of Problem 4 admits a Riemannian description. The orthonormal constraint, $R_i^\top R_i = I_d, R_i \in \mathbb{R}^{p \times d}$, is equivalent to the Stiefel manifold $\mathrm{St}(d, p)$ [8]. Similarly, the l unit-norm constraints, $\|r_{ij}\|_2^2 = 1, r_{ij} \in \mathbb{R}^p$, define the unit-sphere in $\mathbb{R}^p$. Furthermore, the product manifold of l unit spheres can also be expressed as the oblique manifold [44], $\mathrm{OB}(p, l)$, the set of matrices in $\mathbb{R}^{p \times l}$ with unit-norm columns. Finally, the remaining variables are translations, t_i, and are unconstrained vectors and thus are defined by the Euclidean manifold. Therefore, the feasible set of Problem 4 can be expressed as a product of Riemannian manifolds for any p. We describe the corresponding Riemannian optimization problem in Problem 5.

Problem 5 (Problem 4 as Riemannian optimization)**.** *Given the measurements of Problem 1, find the variables,* $\{R_i, t_i\}_{i=1}^n \cup \{r_{ij}\}_{(i,j) \in \mathcal{E}_r}$ *, which solve:*

$$\min_{\substack{R_i \in \mathrm{St}(d,p) \\ t_i \in \mathbb{R}^d \\ r \in \mathrm{OB}(p,l)}} \sum_{(i,j) \in \mathcal{E}_p} \kappa_{ij} \|R_j - R_i \tilde{R}_{ij}\|_F^2$$

$$+ \sum_{(i,j) \in \mathcal{E}_p} \tau_{ij} \left\| t_j - t_i - R_i \tilde{t}_{ij} \right\|_2^2. \quad (16)$$

$$+ \sum_{(i,j) \in \mathcal{E}_r} \frac{1}{\sigma_{ij}^2} \| t_j - t_i - \tilde{r}_{ij} r_{ij} \|_2^2$$

where $\{r_{ij}\}_{(i,j) \in \mathcal{E}_r}$ *are the l unit-norm columns of r.*

We emphasize that Problem 5 is exactly the rank-restricted SDP of Problem 4, reformatted to explicitly state that the feasible set of Problem 4 is a product of Riemannian manifolds.

B. The Riemannian Staircase

The Riemannian staircase approach we use follows the general methodology outlined in [13, Algorithm 1] with slight alterations. Specifically, Riemannian optimization is performed at a given level of relaxation, as determined by p. If the estimate, X^*, is found to be optimal (Algorithm 1) then the algorithm returns the certified solution. If X^* is not found to be optimal, the problem is relaxed by incrementing p and the previous estimate is used to initialize the relaxed problem. As the estimate will be a first-order stationary point if trivially lifted (i.e., if appending a column of zeros to X^*) we perturb the point slightly. This process continues until a certifiably optimal solution is found[3].

The primary differences between our approach and [13, Algorithm 1] are that the previous work (1) was defined solely over Stiefel manifolds of uniform dimension and (2) used rank-deficiency of the estimate to certify the solution. Structural differences between RA-SLAM and [13] drove the need for a novel problem formulation and corresponding certification scheme.

C. Certifiably Correct Estimation

We have now established: a certification scheme, means for lifting the Problem 4 to higher dimensions, and how to represent each lifted relaxation of Problem 4 as a Riemannian optimization problem. We combine these three contributions to

---

[2]The perturbation shifts the lifted solution from a first-order critical point. While we randomly sample the perturbation $\delta \in \mathbb{R}^k$ without observing errors, we note other approaches with theoretical guarantees exist [13, 15].

[3]For similar rank-restricted SDPs there are known bounds on the required p to guarantee convergence (with nuanced caveats regarding the geometry of the SDP) [12, 14]. In practice, these bounds are often well above the level of relaxation required to obtain an optimal solution.

Fig. 2. The equipment used in our marine experiments. (Top) A Jetyak [66], which we refer to as a beacon, equipped with a GPS transponder. (Bottom) Standard watercraft, which we will refer to as Low-Nav craft, equipped with an electric trolling motor, Sparton AHRS-M2 attitude and heading reference system, and GPS transponder. Each platform has a MicroModem-2 [67] and acoustic transducer for inter-platform acoustic ranging and communications.

construct an initialization-independent approach to certifiably correct RA-SLAM (CORA).

Given an initial estimate, X_0, our Riemannian staircase approach is applied to obtain a low-rank, certifiably optimal solution to Problem 3. This SDP solution is projected to the feasible set of the original problem (Problem 1) and the projected solution is refined with local Riemannian optimization. We describe these steps in Algorithm 2.

We note that by obtaining a certifiably optimal solution to Problem 3 we also establish a lower-bound on the optimal value of Problem 1. This lower-bound both provides a means of certification, and an upper-bound on suboptimality should the final estimate not be certifiable.

Additionally, while we find that, in practice, the Riemannian staircase obtains a certifiable solution to Problem 3 regardless of the choice of X_0, we currently lack strict theoretical guarantees for our specific problem (see Footnote 3). Regardless, X_0 affects the practical efficiency of Algorithm 2, as a high-quality initialization can aid in finding certifiable solutions at lower levels of relaxation.

VI. EXPERIMENTS

We present two sets of RA-SLAM experiments: two marine surface vehicles with acoustic ranging and simulated examples with multiple robots. We demonstrate that we are typically able to certify the optimality of our solutions. Furthermore, we identify certain conditions which appear to affect the tightness of the relaxation we pose, suggesting areas of theoretical interest and future investigation.

A. Marine Experiments

The marine experiments were conducted with the platforms described in Fig. 2 over a 250-meter by 100-meter river section. This system was intended as a heterogeneous platform to investigate how agents with high-accuracy navigation (e.g.,

Fig. 3. Certified optimal result from marine acoustic ranging experiments described in Section VI-A. Our estimate of the Low-Nav trajectory (green) closely matches the ground-truth obtained from GPS (red). Similarly, the estimated beacon positions almost exactly match the GPS groundtruth.

GPS or high-cost inertial navigation) could enhance a low-accuracy navigation system. In this experiment the beacon (yellow Jetyak) localizes via GPS fixes at 1 Hz, as proxy for high-accuracy navigation system. In contrast, the Low-Nav craft (blue-white watercraft) obtains odometry by combining heading estimates from a Sparton AHRS-M2 attitude heading reference system with a constant-velocity assumption. The beacon effectively acts as a moving landmark, with a GPS prior on its location and intermittent range measurements to the Low-Nav Craft.

Inter-agent acoustic ranging used two Micromodem-2 systems [67]. Ground-truth vehicle positions were obtained from GPS receivers mounted on each vehicle. The assumed constant velocity was obtained from the average velocity over 10 hand-timed point-to-point 100 meter traverses.

Our estimation problem considers the GPS measurements of the beacon position, inter-agent acoustic ranges, and the constant-velocity odometry. We jointly estimate the pose of the Low-Nav craft and the positions of the beacon. Low-Nav poses are taken at 1 Hz frequency while beacon positions are only considered when new range measurements occur.

As seen in Fig. 3, our method returns a qualitatively correct and certifiably optimal estimate of the Low-Nav and beacon trajectories despite being given a random initialization. We claim this as evidence of robustness of CORA, particularly with respect to the naive odometry model used.

B. Simulated Multirobot Experiments

To empirically characterize our algorithm we simulate 2D multi-robot experiments. We perform parameter sweeps over: the number of robots, ranging sensor noise parameters, number of range measurements, number of pose variables. Default values of 4 robots, $(0.5)^2$ meters squared ranging covariance, 500 range measurements, and 4000 poses were used for each parameter not being swept. For each parameter sweep we ran a scenario with no interrobot relative pose measurements and 100 interrobot relative pose measurements, with notable differences observed between the two.

For each sweep we plot the relative suboptimality, $\frac{f^* - f_l^*}{f_l^*}$, where f^* is the cost of the final estimate and f_l^* is the certified lower bound obtained from CORA. These plots can be observed in Fig. 4.
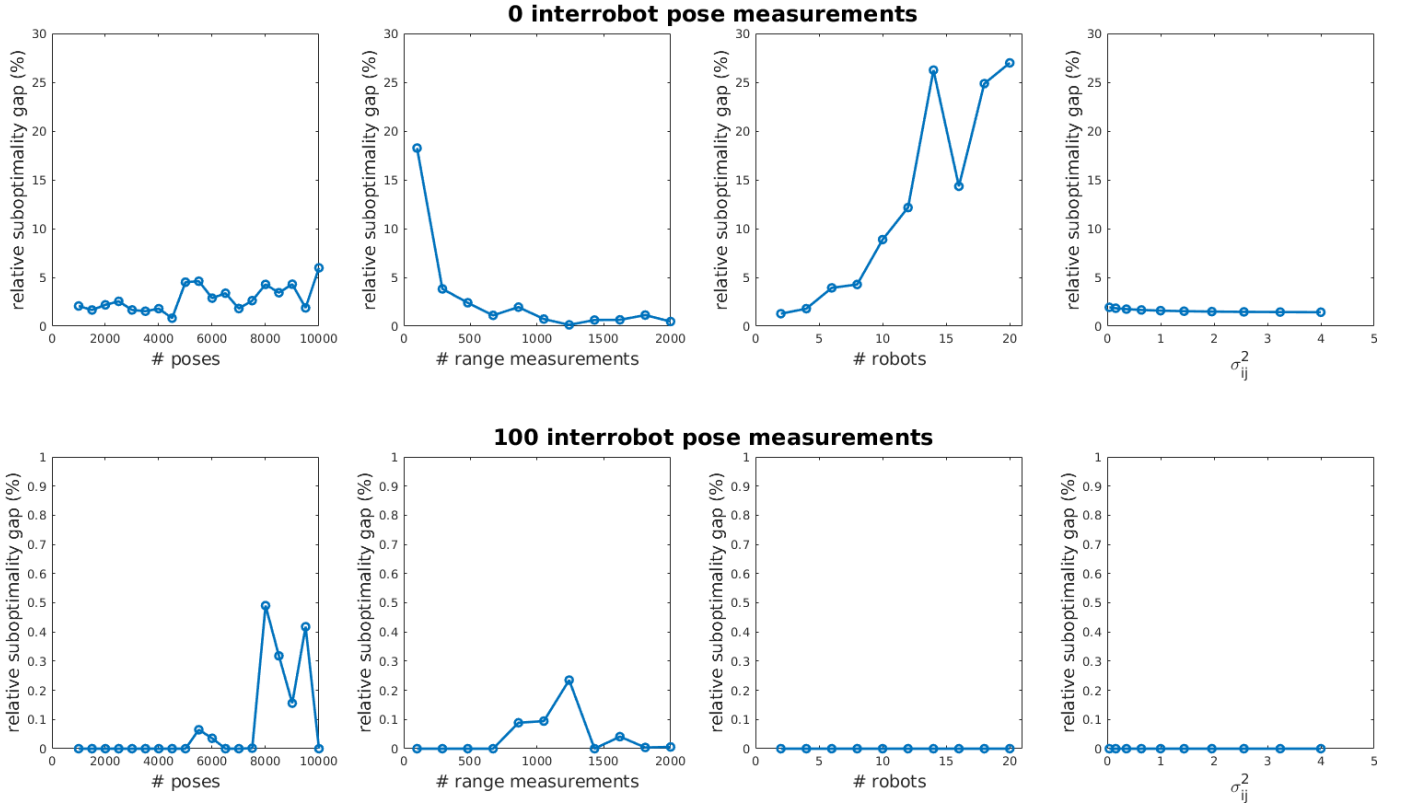
Fig. 4. Comparison of relative suboptimality gaps achieved on different parameter sweeps. There is a substantial effect observed by the insertion of interrobot relative pose measurements. In the case of no relative pose measurements (top row) there are substantially higher suboptimality gaps computed and trends emerge between the suboptimality gap and various parameters. In the case of 100 relative pose measurements (bottom row) we observe suboptimality gaps consistently below 0.5% and can often certify the optimality of the solution (suboptimality is zero).

Number of Robots: We sweep from 2 to 20 robots while maintaining a constant number of total poses. As observed in Fig. 4, the number of robots has a substantial effect on the suboptimality in the case of no interrobot pose measurements. We hypothesize this is because each new robot introduces additional symmetries into the solution, which must be constrained by the relative measurements to other robots. As a single range measurement is not sufficient to fully constrain the relative pose between robots, the cost landscape in this scenario is likely more symmetrical and possibly does not contain a single unique solution. This hypothesis is further supported by the results when 100 relative pose measurements are added, in which suboptimality gap is consistently zero regardless of the number of robots. In this instance, the relative poses are likely fully constrained by the relative pose measurements and the range measurements just further improve the estimate.

Number of Range Measurements: We sweep from 100 to 2000 range measurements. In Fig. 4 we find that, in the case of no interrobot pose measurements, an increase in range measurement density leads to a sharp decrease in the suboptimality gap. This trend is not observed in the case of 100 interrobot pose measurements. We hypothesize this is due to the increased number of measurements reducing the potential symmetries in the cost landscape. Effectively this is the same mechanism we hypothesize caused the trends found as the number of robots increased.

Range Noise Parameters: Furthermore, we sweep over the ranging sensor additive noise covariance, σ_{ij}^2, from $(0.02)^2$ to $(2)^2$. This parameter sweep has a minor, but clear, effect on the relative suboptimality gap in the case of no interrobot pose measurements. Specifically, as the covariance increases the suboptimality gap appears to decrease and approach a clear asymptote. This is likely due to how the range covariance shapes the cost landscape, with range cost scaling as $1/\sigma_{ij}^2$.

Number of Pose Variables: We sweep from 10^3 to 10^4 pose variables. The plots in Fig. 4 suggest that increasing the number of pose variables *may* lead to increasing suboptimality gap. A driving mechanism for this is unclear, but may be due to increased degrees of freedom in the solution. These trends are not as pronounced as in the other observed phenomena.

VII. CONCLUSION

In this work we described CORA, the first algorithm to obtain certifiably optimal RA-SLAM solutions. CORA combines two novel algorithmic capabilities described in this work, (1) a global optimality certification method and (2) a Riemannian staircase methodology for initialization-independent certifiably correct RA-SLAM.

We demonstrated the efficacy of CORA on a real-world experiment utilizing acoustic ranging as well as multiple simulated multi-robot RA-SLAM problems. Notably, in addition to returning solution estimates, CORA obtains an upper bound on

solution suboptimality. We found this bound was often tight, i.e., we obtained solutions with zero suboptimality.

Furthermore, we used this suboptimality bound to empirically observe underlying challenges of RA-SLAM (e.g., potential solution symmetries). These observations point to notable differences between the loss-landscapes of RA-SLAM and pose-graph SLAM problems, which typically admit unique solutions. These unique challenges in RA-SLAM motivate further development of algorithms and analysis, specifically at the intersection of RA-SLAM and the geometry of SDPs.

VIII. ACKNOWLEDGEMENTS

APPENDIX A
VARIABLE AND CONSTRAINT INDEXING

The constructions of Q and A_i require defining specific indices of the matrices. We designate a bijective function, $id : \mathrm{Var} \rightarrow \{1, \ldots, k\}$, mapping each variable to the corresponding row in X. For rotation variables, $id(R_{i,p})$ returns the row index corresponding to the pth column of R_i in X.

APPENDIX B
FORM OF THE DATA MATRIX, Q

Q is a sparse, real, symmetric, positive-semidefinite matrix which encodes the cost of the RA-SLAM problem. We describe Q as the summation of the relative-pose cost terms with the range cost terms, i.e., $Q \triangleq Q_p + Q_r$.

Construction of Q_p follows the approach of [42, Appendix II], which connects Q_p to the graph connection Laplacian.

Constructing Q_r: We first recall the form of the range-cost terms of Problem 2:

$$\sum_{(i,j)\in\mathcal{E}_r} \frac{1}{\sigma_{ij}^2} \|t_j - t_i - \tilde{r}_{ij} r_{ij}\|_2^2 \qquad (17)$$

Without loss of generality, we ignore the weighting term $(1/(\sigma_{ij}^2))$ and expanding Eq. (17) results in:

$$\|t_j\|_2^2 + \|t_i\|_2^2 + \|\tilde{r}_{ij} r_{ij}\|_2^2 \\ - 2\langle t_i, t_j\rangle - 2\langle t_i, \tilde{r}_{ij} r_{ij}\rangle + 2\langle t_j, \tilde{r}_{ij} r_{ij}\rangle. \qquad (18)$$

This can be further expanded to

$$\langle t_j, t_j\rangle + \langle t_i, t_i\rangle + \tilde{r}_{ij}^2 \langle r_{ij}, r_{ij}\rangle \\ - 2\langle t_i, t_j\rangle - 2\tilde{r}_{ij}\langle t_i, r_{ij}\rangle + 2\tilde{r}_{ij}\langle t_j, r_{ij}\rangle, \qquad (19)$$

where $\langle \cdot, \cdot \rangle$ denotes the vector inner product operation. Specifically, the range cost terms are (weighted) sums of the inner products between these variables.

In the form of Problem 4 the range cost is equivalently written as $\mathrm{tr}(QXX^\top)$.

We observe the entries of $XX^\top$ at row p and column q are as follows,

$$XX_{(p,q)}^\top = \langle \mathrm{var}_p, \mathrm{var}_q\rangle, \qquad (20)$$

where var_i is the variable in the i-th row of X. More precisely, $\mathrm{var}_i \triangleq id^{-1}(i)$, where $id^{-1}(\cdot)$ is the inverse of $id(\cdot)$.

As the cost is simply an inner product between Q_r and $XX^\top$, we can consider Q_r as a weighting function over these respective inner products. Furthermore, we can think of Q_r as a sum of matrices, each representing a single measurement. That is,

$$Q_r = \sum_{(i,j)\in\mathcal{E}_r} Q_{r_{ij}}. \qquad (21)$$

As Eq. (19) describes each range term as a weighted sum of inner products, we can thus determine the values at index (p, q) of $Q_{r_{ij}}$ as:

$$Q_{r_{ij}}(p, q) \triangleq \begin{cases} 1, & p = q = i_{t_i} \\ 1, & p = q = i_{t_j} \\ \tilde{r}_{ij}^2, & p = q = i_{r_{ij}} \\ -1, & (p, q) = (i_{t_i}, i_{t_j}) \text{ or } (i_{t_j}, i_{t_i}) \\ -\tilde{r}_{ij}, & (p, q) = (i_{t_i}, i_{r_{ij}}) \text{ or } (i_{r_{ij}}, i_{t_i}) \\ \tilde{r}_{ij}, & (p, q) = (i_{t_j}, i_{r_{ij}}) \text{ or } (i_{r_{ij}}, i_{t_j}) \end{cases} \qquad (22)$$

where we use the shorthands $i_{t_i} \triangleq id(t_i)$, $i_{t_i} \triangleq id(t_j)$, $i_{r_{ij}} \triangleq id(r_{ij})$. To recover the weighting term, each resulting $Q_{r_{ij}}$ can be multiplied by the respective $1/(\sigma_{ij}^2)$.

APPENDIX C
DEFINING THE CONSTRAINTS, A_i

We give the form of the various constraint matrices, A_i, in Problem 4. These matrices – particularly the sparsity patterns of these matrices – are the central objects in our subsequent demonstration that the linear independence constraint qualification (LICQ) is satisfied for our problem. While we prove the LICQ for Problem 4, we point to Problem 2, to observe that the constraints are naturally sorted into two sets: orthonormal ($\mathbf{A}_{\mathrm{orth}}$) and distance constraints ($\mathbf{A}_{\mathrm{dist}}$).

Orthonormal Constraints: Inspection of $XX^\top$ reveals that the $R_i^\top R_i$ entries exist as symmetric, block-diagonal values. To enforce the constraint $R_i^\top R_i = I_d$ each unique entry must be independently constrained, and as $R_i^\top R_i$ is symmetric there are only $d(d+1)/2$ constraints on its elements, corresponding to the number of elements in its upper triangle. The orthonormal constraint matrices differ by whether they represent a constraint on a diagonal or off-diagonal element of $R_i^\top R_i$

We define the constraint matrix $A_{i,p,p} \in \mathbb{R}^{k \times k}$, corresponding to the pth diagonal entry of $R_i^\top R_i$, as follows:

$$A_{i,p,p} = \begin{cases} 1, & id(R_{i,p})\text{-th diagonal} \\ 0, & \text{otherwise} \end{cases} . \quad (23)$$

The corresponding right-hand side, $b_{i,p,p}$, is equal to 1.

Next, we define the matrix $A_{i,p,q} \in \mathbb{R}^{k \times k}$, corresponding to the off-diagonal entry at row p and column q of $R_i^\top R_i$, as follows:

$$A_{i,p,q} = \begin{cases} 1/2, & \text{row} = id(R_{i,p}), \ \text{col} = id(R_{i,q}) \\ 1/2, & \text{row} = id(R_{i,q}), \ \text{col} = id(R_{i,p}) \\ 0, & \text{otherwise} \end{cases} . \quad (24)$$

The corresponding right-hand side, $b_{i,p,q}$, is equal to 0.

Distance Constraints: Each distance constraint is a unit-norm constraint on a single variable (r_{ij}), the corresponding constraint matrix ($A_{r_{ij}}$) is thus as follows:

$$A_{r_{ij}} = \begin{cases} 1, & id(r_{ij})\text{-th diagonal} \\ 0, & \text{otherwise} \end{cases} . \quad (25)$$

The corresponding right-hand side, $b_{r_{ij}}$, is 1.

Appendix D
The Linear Independence Constraint Qualification

Within this appendix we prove the statement of Theorem 1, namely that the LICQ is satisfied for any feasible point of Problem 4. The LICQ is a statement of the gradients of the problem constraints.

To simplify notation, we respectively use $\nabla \mathbf{A}_{\text{orth}}$ and $\nabla \mathbf{A}_{\text{dist}}$ to refer to the set of constraint gradients defined by $\mathbf{A}_{\text{orth}}$ and $\mathbf{A}_{\text{dist}}$ (see Section C). E.g., $\nabla \mathbf{A}_{\text{orth}} = \{A_i X^*, A_i \in \mathbf{A}_{\text{orth}}\}$.

To prove Theorem 1, we first separately prove linear independence for $\nabla \mathbf{A}_{\text{orth}}$ and $\nabla \mathbf{A}_{\text{dist}}$ for any Problem 4 feasible point. We then show that, by construction, $\nabla \mathbf{A}_{\text{orth}}$ and $\nabla \mathbf{A}_{\text{dist}}$ span complementary vector spaces. Finally, we apply the fact that the union of two linearly independent sets over complementary vector spaces is linearly independent to prove that the LICQ is always satisfied for any feasible point in Problem 4.

Lemma 2 (Linear independence of orthonormality constraint gradients). *The set of gradients of the orthonormality constraints, $\nabla \mathbf{A}_{orth} = \{A_i X^* | A_i \in \mathbf{A}_{orth}\}$, of Problem 4 is a linearly independent set for any feasible point, X^*, in Problem 4.*

Proof: we prove that $\nabla \mathbf{A}_{\text{orth}}$ is an independent set by demonstrating that the constraint gradients are orthogonal to each other. We demonstrate that the constraint gradients are nonzero for any feasible X^*. As the gradients are nonzero, if they are orthogonal they must have inner product, $\langle A, B \rangle = \text{tr}(B^\top A)$, of zero.

Direct computation of $A_{i,p,q} X^*$ obtains,

$$A_{i,p,q} X^* = \begin{cases} (1/2) X^*_{id(R_{i,q})}, & \text{row} = id(R_{i,p}) \\ (1/2) X^*_{id(R_{i,p})}, & \text{row} = id(R_{i,q}) \\ 0, & \text{otherwise} \end{cases} , \quad (26)$$

where $X^*_{id(R_{i,p})}$ is the $id(R_{i,p})$-th row of X^*.

In the case of $p = q$ these two terms sum such that the resulting product is,

$$A_{i,p,p} X^* = \begin{cases} X^*_{id(R_{i,p})}, & \text{row} = id(R_{i,p}) \\ 0, & \text{otherwise} \end{cases} . \quad (27)$$

As X^* is a feasible point to problem Problem 2, $X^*_{id(R_{i,p})}$ must be unit norm. Therefore, any orthonormality constraint gradient must be nonzero.

For any pair of two unique orthonormality constraint matrices, $A_{i,p,q}$ and $A_{j,r,s}$, there are three possible cases:

1) the rotations are different ($i \neq j$)
2) the rotations are the same but the rotation sub-indices are entirely different ($i = j, p \neq r, q \neq s$)
3) the rotations are the same and a single pair of sub-indices is the same ($i = j, p = r$ or $q = s$).

For cases 1 and 2 $\langle A_{i,p,q} X^*, A_{j,r,s} X^* \rangle$ must be zero, as the two constraint gradients will have entirely separate nonzero rows (Eq. (26)).

Now we show that in case 3, the inner product is zero for any feasible point (i.e., any point satisfying $R_i^\top R_i = I_d$). As the constraint matrices are symmetric, without loss of generality we assume that the overlapping indices are p and r. Drawing from the form of the orthonormality constraint gradients in Eq. (26), we observe that:

$$\begin{aligned} &\langle A_{i,p,q} X^*, A_{i,p,s} X^* \rangle \\ \propto \ &\langle R_{i,s}, R_{i,q} \rangle \\ = \ &(R_{i,s}^\top) R_{i,q} \end{aligned} , \quad (28)$$

where, $\propto$ indicates two terms are proportional up to a scalar constant and $R_{i,s}$ is the s-th column of R_i. The proportionality comes into play as the entries of the gradients may be scaled by $(1/2)$ per Eq. (26). As all R_i are constrained to be orthonormal, for any feasible point this inner product must be zero.

As a result, for any Problem 4 feasible point, the gradients of all orthonormality constraints are orthogonal. Therefore, $\nabla \mathbf{A}_{\text{orth}}$ must be linearly independent. ∎

Lemma 3 (Linear independence of distance constraint gradients). *The gradients of the unit-ball constraints, $\nabla \mathbf{A}_{dist} = \{A_{r_{ij}} X^* | A_{r_{ij}} \in \mathbf{A}_{orth}\}$, of Problem 4 is a linearly independent set.*

Proof: Computation of $A_{r_{ij}}X^*$ attains,

$$A_{r_{ij}}X^* = \begin{cases} r_{ij}^*, & \text{row} = id(r_{ij}) \\ 0, & \text{otherwise} \end{cases} \tag{29}$$

where r_{ij}^* is the estimate of the variable r_{ij} contained in X^*. For any feasible point X^* to Problem 4, $\|r_{ij}^*\|_2$ must be 1.

Therefore, each unit-ball constraint gradient, $A_{r_{ij}}X^*$, must have nonzero components in its $id(r_{ij})$-th row and nowhere else. As there is only one constraint per each r_{ij}, no two unit-ball constraint gradients have overlapping nonzero entries. Therefore, the gradients of all unit-ball constraints are orthogonal to each other. As all gradients are orthogonal and nonzero, $\nabla \mathbf{A}_{\text{dist}}$ must be linearly independent. ∎

Lemma 4 (Complementarity of Constraint Gradients). $\nabla \mathbf{A}_{orth} \cap \nabla \mathbf{A}_{dist} = \{0\}$

Proof: We draw on the forms of the orthonormality constraint gradients (Eq. (26)) and the unit-ball constraint gradients (Eq. (29)).

The nonzero rows of $\nabla \mathbf{A}_{\text{orth}}$ correspond to the indices of all rotation variables, $\{id(R_{i,p}), \ i = 1, \ldots, n \text{ and } p = 1, \ldots, d\}$. Similarly, the nonzero rows of $\nabla \mathbf{A}_{\text{dist}}$ correspond to the indices of all distance variables, $\{id(r_{ij}) \mid r_{ij} \in \mathcal{E}_r\}$.

The set of rotation variables, $\{R_i, \ i = 1, \ldots, n\}$, is disjoint to the set of distance variables, $\{r_{ij} \mid r_{ij} \in \mathcal{E}_r\}$. Observe that the sets of nonzero rows of each set of constraints result from applying $id(\cdot)$ to the respective variables.

As $id(\cdot)$ is bijective, and the sets of variables are disjoint, the sets of nonzero rows of $\nabla \mathbf{A}_{\text{orth}}$ and $\nabla \mathbf{A}_{\text{dist}}$ must also be disjoint. Therefore, the linear spaces spanned by $\nabla \mathbf{A}_{\text{orth}}$ and $\nabla \mathbf{A}_{\text{dist}}$ have no common nonzero entries and $\nabla \mathbf{A}_{\text{orth}} \cap \nabla \mathbf{A}_{\text{dist}} = \{0\}$. ∎

Finally, we prove the LICQ is satisfied for all feasible points of Problem 4.

Proof of Theorem 1: By Lemma 2 and Lemma 3, for any feasible point of Problem 4 the sets $\nabla \mathbf{A}_{\text{orth}}$ and $\nabla \mathbf{A}_{\text{dist}}$ are each linearly independent. Additionally, by Lemma 4, $\nabla \mathbf{A}_{\text{orth}} \cap \nabla \mathbf{A}_{\text{dist}} = \{0\}$. As each set is linearly independent when evaluated at a feasible point of Problem 4 and $\nabla \mathbf{A}_{\text{orth}} \cap \nabla \mathbf{A}_{\text{dist}} = \{0\}$, the union of these sets, $\nabla \mathbf{A}_{\text{orth}} \cup \nabla \mathbf{A}_{\text{dist}}$, is a linearly independent set for any feasible point of Problem 4. Therefore, for any feasible point of Problem 4 the set of all constraint gradients is linearly independent. ∎

REFERENCES

[1] Jesse R. Pelletier, Brendan W. O'Neill, John J. Leonard, Lee Freitag, and Eric Gallimore. AUV-assisted diver navigation. *IEEE Robotics and Automation Letters*, 7 (4):10208–10215, 2022. ISSN 23773766. doi: 10.1109/ LRA.2022.3191164.

[2] Liam Paull, Sajad Saeedi, Mae Seto, and Howard Li. AUV navigation and localization: A review. *Oceanic Engineering, IEEE Journal of*, 39(1):131–149, 2014.

[3] Kexin Guo, Zhirong Qiu, Wei Meng, Lihua Xie, and Rodney Teo. Ultra-wideband based cooperative relative localization algorithm and experiments for multiple unmanned aerial vehicles in GPS denied environments. *International Journal of Micro Air Vehicles*, 9(3):169–186, 2017. ISSN 17568307. doi: 10.1177/1756829317695564.

[4] Nobuhiro Funabiki, Benjamin Morrell, Jeremy Nash, and Ali Akbar Agha-Mohammadi. Range-aided posegraph-based SLAM: Applications of deployable ranging beacons for unknown environment exploration. *IEEE Robotics and Automation Letters*, 6(1):48–55, 2021. ISSN 23773766. doi: 10.1109/LRA.2020.3026659.

[5] Elizabeth R Boroson, Robert Hewitt, Nora Ayanian, and Jean-pierre De Croix. Inter-robot range measurements in pose graph optimization. *2020 IEEE/RSJ International Conference on Intelligent Robots and Systems (IROS)*, pages 4806–4813, 2020.

[6] C. D. Cadena Lerma, L. Carlone, H. Carrillo, Y. Latif, D. Scaramuzza, J. Neira, I. Reid, and J. Leonard. Past, present, and future of simultaneous localization and mapping: Towards the robust-perception age. *IEEE Trans. Robotics*, 2016.

[7] David M. Rosen, Kevin J. Doherty, Antonio Terán Espinoza, and John J. Leonard. Advances in inference and representation for simultaneous localization and mapping. *Annual Review of Control, Robotics, and Autonomous Systems*, 4(1):215–242, 2021. ISSN 2573-5144. doi: 10.1146/annurev-control-072720-082553.

[8] David M. Rosen, Luca Carlone, Afonso S. Bandeira, and John J. Leonard. SE-Sync: A certifiably correct algorithm for synchronization over the special Euclidean group. *The International Journal of Robotics Research*, 38(2-3):95–125, 2019. ISSN 17413176. doi: 10.1177/ 0278364918784361.

[9] F. Dellaert and M. Kaess. Square Root SAM: Simultaneous localization and mapping via square root information smoothing. *Intl. J. of Robotics Research*, 25(12):1181–1203, December 2006.

[10] M. Kaess, A. Ranganathan, and F. Dellaert. iSAM: Incremental smoothing and mapping. *IEEE Trans. Robotics*, 24(6):1365–1378, December 2008.

[11] Samuel Burer and Renato DC Monteiro. A nonlinear programming algorithm for solving semidefinite programs via low-rank factorization. *Mathematical Programming*, 95(2):329–357, 2003.

[12] Samuel Burer and Renato DC Monteiro. Local minima and convergence in low-rank semidefinite programming. *Mathematical programming*, 103(3):427–444, 2005.

[13] Nicolas Boumal. A Riemannian low-rank method for optimization over semidefinite matrices with block-diagonal constraints. pages 1–36, 2015. URL http://arxiv.org/abs/ 1506.00575.

[14] Nicolas Boumal, Vladislav Voroninski, and Afonso S. Bandeira. The non-convex Burer-Monteiro approach works on smooth semidefinite programs. *Advances in Neural Information Processing Systems*, (Nips):2765–2773, 2016. ISSN 10495258.

[15] David M. Rosen. Scalable low-rank semidefinite pro-

gramming for certifiably correct machine perception. pages 551–566, 2020. ISSN 25111264. doi: 10.1007/978-3-030-66723-8_33.

[16] Timothy D Barfoot. *State Estimation for Robotics*. Cambridge University Press, 2017.

[17] Afonso S Bandeira. A note on probably certifiably correct algorithms. *Comptes Rendus Mathematique*, 354 (3):329–333, 2016.

[18] V. Jeyakumar, A. M. Rubinov, and Z. Y. Wu. Non-convex quadratic minimization problems with quadratic constraints: Global optimality conditions. *Mathematical Programming*, 110(3):521–541, 2007. ISSN 00255610. doi: 10.1007/s10107-006-0012-5.

[19] Guoyin Li. Global quadratic minimization over bivalent constraints: Necessary and sufficient global optimality condition. *Journal of Optimization Theory and Applications*, 152(3):710–726, 2012. ISSN 15732878. doi: 10.1007/s10957-011-9930-3.

[20] Yulun Tian, Kasra Khosoussi, David M Rosen, and Jonathan P How. Distributed certifiably correct pose-graph optimization. *IEEE Transactions on Robotics*, 37 (6):2137–2156, 2021.

[21] José Pedro Iglesias, Carl Olsson, and Fredrik Kahl. Global optimality for point set registration using semidefinite programming. *Proceedings of the IEEE Computer Society Conference on Computer Vision and Pattern Recognition*, pages 8284–8292, 2020. ISSN 10636919. doi: 10.1109/CVPR42600.2020.00831.

[22] Heng Yang, Jingnan Shi, and Luca Carlone. TEASER: Fast and certifiable point cloud registration. *IEEE Transactions on Robotics*, pages 1–44, 2020. ISSN 19410468. doi: 10.1109/TRO.2020.3033695.

[23] Mercedes Garcia-Salguero, Jesus Briales, and Javier Gonzalez-Jimenez. Certifiable relative pose estimation. *Image and Vision Computing*, 109, 2021. ISSN 02628856. doi: 10.1016/j.imavis.2021.104142.

[24] Jesus Briales and Javier Gonzalez-Jimenez. Fast global optimality verification in 3D SLAM. *IEEE International Conference on Intelligent Robots and Systems*, pages 4630–4636, 2016. ISSN 21530866. doi: 10.1109/IROS.2016.7759681.

[25] Luca Carlone, David M. Rosen, Giuseppe Calafiore, John J. Leonard, and Frank Dellaert. Lagrangian duality in 3D SLAM: Verification techniques and optimal solutions. *IEEE International Conference on Intelligent Robots and Systems*, 2015-Decem:125–132, 2015. ISSN 21530866. doi: 10.1109/IROS.2015.7353364.

[26] Frederike Dümbgen, Connor Holmes, and Timothy D. Barfoot. Safe and smooth: Certified continuous-time range-only localization. *IEEE Robotics and Automation Letters*, 2022. URL http://arxiv.org/abs/2209.04266.

[27] Mercedes Garcia-Salguero and Javier Gonzalez-Jimenez. A sufficient condition of optimality for the relative pose problem between cameras. *SIAM Journal on Imaging Sciences*, 14(4):1617–1634, 2021. doi: 10.1137/21m1397970.

[28] Richard Hartley, Fredrik Kahl, Carl Olsson, and Yong-duek Seo. Verifying global minima for L2 minimization problems in multiple view geometry. *International Journal of Computer Vision*, 101(2):288–304, 2013. ISSN 09205691. doi: 10.1007/s11263-012-0569-9.

[29] Carl Olsson, Fredrik Kahl, and Richard Hartley. Projective least-squares: Global solutions with local optimization. *2009 IEEE Conference on Computer Vision and Pattern Recognition, CVPR 2009*, pages 1216–1223, 2009. doi: 10.1109/CVPRW.2009.5206864.

[30] Xiaowei Bao, Nikolaos V. Sahinidis, and Mohit Tawarmalani. Semidefinite relaxations for quadratically constrained quadratic programming: A review and comparisons. *Mathematical Programming*, 129(1): 129–157, 2011. ISSN 00255610. doi: 10.1007/s10107-011-0462-2.

[31] Jesus Briales and Javier Gonzalez-Jimenez. Convex global 3D registration with Lagrangian duality. *Proceedings - 30th IEEE Conference on Computer Vision and Pattern Recognition, CVPR 2017*, 2017-Janua:5612–5621, 2017. doi: 10.1109/CVPR.2017.595.

[32] Carl Olsson and Anders Eriksson. Solving quadratically constrained geometrical problems using Lagrangian duality. *Proceedings - International Conference on Pattern Recognition*, 2008. ISSN 10514651. doi: 10.1109/icpr.2008.4761896.

[33] Yuehaw Khoo and Ankur Kapoor. Non-iterative rigid 2D/3D point-set registration using semidefinite programming. *IEEE Transactions on Image Processing*, 25(7): 2956–2970, 2016. ISSN 10577149. doi: 10.1109/TIP.2016.2540810.

[34] Heng Yang and Luca Carlone. A polynomial-time solution for robust registration with extreme outlier rates. *Robotics: Science and Systems*, (Section IV), 2019. ISSN 2330765X. doi: 10.15607/RSS.2019.XV.003.

[35] Jesus Briales, Laurent Kneip, and Javier Gonzalez-Jimenez. A certifiably globally optimal solution to the non-minimal relative pose problem. In *Proceedings of the IEEE Computer Society Conference on Computer Vision and Pattern Recognition*, pages 145–154, 2018. ISBN 9781538664209. doi: 10.1109/CVPR.2018.00023.

[36] Mercedes Garcia-Salguero, Jesus Briales, and Javier Gonzalez-Jimenez. A tighter relaxation for the relative pose problem between cameras. *Journal of Mathematical Imaging and Vision*, 64(5):493–505, 2022. ISSN 15737683. doi: 10.1007/s10851-022-01085-z. URL https://doi.org/10.1007/s10851-022-01085-z.

[37] Chris Aholt, Sameer Agarwal, and Rekha Thomas. A QCQP approach to triangulation. *Lecture Notes in Computer Science (including subseries Lecture Notes in Artificial Intelligence and Lecture Notes in Bioinformatics)*, 7572 LNCS(PART 1):654–667, 2012. ISSN 03029743. doi: 10.1007/978-3-642-33718-5_47.

[38] Yingjian Wang, Xiangyong Wen, Longji Yin, Chao Xu, Yanjun Cao, and Fei Gao. Certifiably optimal mutual localization with anonymous bearing measurements.

[39] Ji Zhao. An efficient solution to non-minimal case essential matrix estimation. *IEEE Transactions on Pattern Analysis and Machine Intelligence*, 44(4):1–1, 2020. ISSN 0162-8828. doi: 10.1109/tpami.2020.3030161.

[40] Luca Carlone, Giuseppe C. Calafiore, Carlo Tommolillo, and Frank Dellaert. Planar pose graph optimization: Duality, optimal solutions, and verification. *IEEE Transactions on Robotics*, 32(3):545–565, 2016. ISSN 15523098. doi: 10.1109/TRO.2016.2544304.

[41] Matthew Giamou, Ziye Ma, Valentin Peretroukhin, and Jonathan Kelly. Certifiably globally optimal extrinsic calibration from per-sensor egomotion. *IEEE Robotics and Automation Letters*, 4(2):367–374, 2019. ISSN 23773766. doi: 10.1109/LRA.2018.2890444Y.

[42] Jesus Briales and Javier Gonzalez-Jimenez. Cartan-sync: Fast and global SE(d)-synchronization. *IEEE Robotics and Automation Letters*, 2(4):2127–2134, 2017. ISSN 23773766. doi: 10.1109/LRA.2017.2718661.

[43] Taosha Fan, Hanlin Wang, Michael Rubenstein, and Todd Murphey. CPL-SLAM: Efficient and certifiably correct planar graph-based SLAM using the complex number representation. *IEEE Transactions on Robotics*, 36:1719—-1737, 2020. URL http://arxiv.org/abs/2007.06708.

[44] Trevor Halsted and Mac Schwager. The Riemannian elevator for certifiable distance-based localization. *Preprint*, 2022. Accessed: Jan. 20, 2023. [Online] Available https://msl.stanford.edu/papers/halsted_riemannian_2022.pdf.

[45] David R Morrison, Sheldon H Jacobson, Jason J Sauppe, and Edward C Sewell. Branch-and-bound algorithms: A survey of recent advances in searching, branching, and pruning. *Discrete Optimization*, 19:79–102, 2016.

[46] David Cox, John Little, and Donal OShea. *Ideals, varieties, and algorithms: an introduction to computational algebraic geometry and commutative algebra*. Springer Science & Business Media, 2013.

[47] Faraz M. Mirzaei and Stergios I. Roumeliotis. Optimal estimation of vanishing points in a Manhattan world. *Proceedings of the IEEE International Conference on Computer Vision*, pages 2454–2461, 2011. doi: 10.1109/ICCV.2011.6126530.

[48] Henrik Stewénius, Frederik Schaffalitzky, and David Nistér. How hard is 3-view triangulation really? *Proceedings of the IEEE International Conference on Computer Vision*, I:686–693, 2005. doi: 10.1109/ICCV.2005.115.

[49] Nikolas Trawny and Stergios I Roumeliotis. On the global optimum of planar, range-based robot-to-robot relative pose estimation. In *2010 IEEE International Conference on Robotics and Automation*, pages 3200–3206. IEEE, 2010.

[50] Faraz M. Mirzaei and Stergios I. Roumeliotis. Globally optimal pose estimation from line correspondences. *Proceedings - IEEE International Conference on Robotics and Automation*, pages 5581–5588, 2011. ISSN 10504729. doi: 10.1109/ICRA.2011.5980272.

[51] Jean-Charles Bazin, Yongduek Seo, and Marc Pollefeys. Globally optimal consensus set maximization through rotation search. In *Asian Conference on Computer Vision*, pages 539–551. Springer, 2012.

[52] Carl Olsson, Fredrik Kahl, and Magnus Oskarsson. Branch-and-bound methods for Euclidean registration problems. *IEEE Transactions on Pattern Analysis and Machine Intelligence*, 31(5):783–794, 2009. ISSN 01628828. doi: 10.1109/TPAMI.2008.131.

[53] Gregory Izatt, Hongkai Dai, and Russ Tedrake. Globally optimal object pose estimation in point clouds with mixed-integer programming. *Springer Proceedings in Advanced Robotics*, 10:695–710, 2020. ISSN 25111264. doi: 10.1007/978-3-030-28619-4_49.

[54] Jiaolong Yang, Hongdong Li, Dylan Campbell, and Yunde Jia. Go-ICP: A globally optimal solution to 3D ICP point-set registration. *IEEE Transactions on Pattern Analysis and Machine Intelligence*, 38(11):2241–2254, 2016. ISSN 01628828. doi: 10.1109/TPAMI.2015.2513405.

[55] Jean-Charles Bazin, Yongduek Seo, Richard Hartley, and Marc Pollefeys. Globally optimal inlier set maximization with unknown rotation and focal length. In *European Conference on Computer Vision*, pages 803–817. Springer, 2014.

[56] Dylan Campbell, Lars Petersson, Laurent Kneip, and Hongdong Li. Globally-optimal inlier set maximisation for simultaneous camera pose and feature correspondence. In *Proceedings of the IEEE International Conference on Computer Vision*, pages 1–10, 2017.

[57] Johan Fredriksson, Viktor Larsson, Carl Olsson, and Fredrik Kahl. Optimal relative pose with unknown correspondences. *Proceedings of the IEEE Computer Society Conference on Computer Vision and Pattern Recognition*, 2016-Decem:1728–1736, 2016. ISSN 10636919. doi: 10.1109/CVPR.2016.191.

[58] Richard I. Hartley and Fredrik Kahl. Global optimization through rotation space search. *International Journal of Computer Vision*, 82(1):64–79, 2009. ISSN 15731405. doi: 10.1007/s11263-008-0186-9.

[59] Laurent Kneip and Simon Lynen. Direct optimization of frame-to-frame rotation. *Proceedings of the IEEE International Conference on Computer Vision*, pages 2352–2359, 2013. doi: 10.1109/ICCV.2013.292.

[60] Fangfang Lu and Richard Hartley. A fast optimal algorithm for L2 triangulation. *Lecture Notes in Computer Science (including subseries Lecture Notes in Artificial Intelligence and Lecture Notes in Bioinformatics)*, 4844 LNCS(PART 2):279–288, 2007. ISSN 16113349. doi: 10.1007/978-3-540-76390-1_28.

[61] Alan Papalia, Joseph Morales, Kevin J Doherty, David M Rosen, and John J Leonard. SCORE: A second-order conic initialization for range-aided SLAM. *arXiv preprint arXiv:2210.03177*, 2022.

[62] Roberto Tron, David M Rosen, and Luca Carlone. On the inclusion of determinant constraints in lagrangian duality for 3d slam. *Proc. Robotics: Science and Systems (RSS),*

Workshop "The Problem of Mobile Sensors", 2(1), 2015.

[63] Naum Z Shor. Quadratic optimization problems. *Soviet Journal of Computer and Systems Sciences*, 25:1–11, 1987.

[64] Gerd Wachsmuth. On LICQ and the uniqueness of Lagrange multipliers. *Operations Research Letters*, 41 (1):78–80, 2013.

[65] Jorge Nocedal and Stephen Wright. *Numerical optimization*. Springer, 1999.

[66] Peter Kimball, John Bailey, Sarah Das, Rocky Geyer, Trevor Harrison, Clay Kunz, Kevin Manganini, Ken Mankoff, Katie Samuelson, Thomas Sayre-McCord, et al. The WHOI Jetyak: An autonomous surface vehicle for oceanographic research in shallow or dangerous waters. In *Autonomous Underwater Vehicles (AUV), 2014 IEEE/OES*, pages 1–7. IEEE, 2014.

[67] E. Gallimore, J. Partan, I. Vaughn, S. Singh, J. Shusta, and L. Freitag. The WHOI micromodem-2: A scalable system for acoustic communications and networking. In *Proc. of the IEEE/MTS OCEANS Conf. and Exhibition*, pages 1 –7, Sep. 2010.